Appl. Phys. A 69, 497–501 (1999) / Digital Object Identifier (DOI) 10.1007/s003399900136

Applied Physics A
Materials
Science & Processing

The emission of correlated electrons from surfaces

J. Berakdar

Max-Planck-Institut für Mikrostrukturphysik, Weinberg 2, 06120 Halle, Germany
(E-mail: jber@mpi-halle.de)

Received: 23 March 1999/Accepted: 25 June 1999/Published online: 23 September 1999

Abstract. This work offers a theoretical framework for the treatment of the simultaneous many-electron excitation in solids and surfaces. Starting from the transition operator, an expansion is presented that treats all involved interactions on equal footing. The method is applied to the simultaneous two-orbital excitation and the results are compared with recent experimental findings. It is concluded that such studies provide a useful tool for the investigation of inter-electronic coupling.

PACS: 79.20.Kz

One of the outstanding problems of theoretical physics is the treatment of correlated many-body electronic systems. In addition to the inherent non-separability of many-body Coulombic systems, the fermionic nature of the electrons and the infinite range of the Coulomb potentials are major obstacles for such a treatment. The theoretical models put forward to deal with this problem can be roughly divided into two categories: (a) first-principles methods and (b) model Hamiltonian approaches. In the first case a "large-molecule approach" is adopted by restricting the number of interacting particles [1] or the inter-electronic coupling is expressed in terms of an effective self-consistent potential, as done in the density functional theory (DFT) [2]. The model Hamiltonian methods, for example the Hubbard and Anderson models [3, 4], proved very useful for the understanding of the physical phenomena that are influenced by the electronic correlation, for example the correlation gap, magnetic exchange and superexchange. The values for the model-dependent key parameters, such as the correlation energy and the charge-transfer energy, can be estimated from spectroscopic data as deduced from Auger and photoemission measurements [5–8]. On the other hand it is well established that the major structure of the output of these experiments can be explained within a single "quasi-particle" picture (see [9] and references therein). Experimental evidence for inter-electronic coupling shows up as subsidiary features in the spectra. Thus, it seems desirable to develop experimental and theoretical techniques whose output can be directly linked to the inter-electronic coupling. Here we suggest the use of the two-electron coincidence spectroscopy.

In this method the energy and angular distributions of two emitted electrons are simultaneously recorded after the absorption of a VUV [10] photon or after a definite energy and momentum loss of an impinging electron [11–17]. The mechanisms leading to the double-electron emission are heavily dependent on the internal coupling between these two electrons. In fact, the simultaneous two-orbital excitation following the absorption of one VUV photon is exclusively caused by the interelectronic interaction. This is due to the single-particle nature of the electric dipole transitions which implies that the photon can only interact with one electron at a time. The second electron is emitted by means of correlation with the first one [18]. Obviously, the probability for the double photoemission (DPE) is much lower than that for the direct single-photoemission which makes the DPE experiment particularly challenging. In fact, it is only very recently that the DPE signal can be experimentally extracted [10] from the large background of uncorrelated secondary electrons. As will be shown below, the two-electron emission upon electron impact is also highly sensitive to the details of the electron–electron coupling.

For the theoretical treatment of the two-electron excitation process the description of the propagation of correlated systems in a multi-center potential (the crystal potential) is indispensable. In the first section of this work we develop therefore a systematic framework for the propagation of correlated compounds under the action of a non-overlapping muffin-tin crystal potential. This provides a calculational scheme for the amplitudes of the correlated electron-pair scattering from a crystal potential. Numerical results are compared with recent experimental data and manifestations of the electronic correlation in the two-electron spectra are pointed out. Unless otherwise stated, atomic units are used throughout.

1 Formal developments

To introduce the notation and the mathematical tools, it is useful to recall briefly the theoretical treatment of the single-particle scattering from a multi-center potential. This for-

mulation is then generalized to the scattering of correlated compounds from a multi-center pontential.

We consider a system, characterized by a Hamiltonian h_0, to be prepared in a well-defined state $|\varphi\rangle$. Under the action of an external perturbation W, the system goes over into the state $|\psi^{\pm}\rangle$ where

$$|\psi^{\pm}\rangle = \left[\mathbf{1} + g_0^{\pm} T^{\pm}\right] |\varphi\rangle \,. \tag{1}$$

Here g_0^+ (g_0^-) is the advanced (retarded) Green function of the reference Hamiltonian h_0. The dynamic response of the system upon the action of W is described by the transition matrix T that satisfies the integral equation

$$T^{\pm} = W + W g_0^{\pm} T^{\pm} \,. \tag{2}$$

The prime focus of this work is to find tractable and reasonable solutions of (2) for interacting many-body systems. As we are concerned with the propagation of correlated systems in ordered materials we analyze the case where W is a crystal potential consisting of a superposition of M individual non-overlapping (ionic core) potentials, w_i, centered at sites $\boldsymbol{R}_i$ with domains Ω_i (in configuration space), i.e.

$$W = \sum_i^M w_i, \;\; \Omega_i \cap \Omega_j = 0, \;\; \forall j \neq i \,. \tag{3}$$

According to the superposition (3), the T operator is decomposed into (for brevity we omit the superscripts)

$$T = \sum_i^M Q_i \,, \tag{4}$$

where

$$Q_i = w_i + w_i g_0 T = w_i + w_i g_0 Q_i + \sum_{j \neq i}^M w_i g_0 Q_j \,. \tag{5}$$

Introducing the single-site transition operator $t_i = w_i + w_i g_0 t_i$, (5) can be rewritten as

$$Q_i = t_i + \sum_{j \neq i}^M t_i g_0 Q_j \,. \tag{6}$$

The T matrix can then be expressed in terms of t_i:

$$T = \sum_i^M t_i + \sum_{j \neq i}^M t_i g_0 (t_j + w_j g_0 T) \,. \tag{7}$$

Now we use the *scattering path operators*, τ^{ij}, as introduce by Gyorffy [19, 20],

$$\tau^{ij} = t_i \delta_{ij} + \sum_{k \neq i}^M t_j g_0 \tau^{ik} = t_i \delta_{ij} + \sum_{k \neq j}^M \tau^{ik} g_0 t_j \,, \tag{8}$$

and sum over j. Comparison with (6) leads to

$$Q_i = \sum_j \tau^{ij} \,, \tag{9}$$

$$T = \sum_i Q_i = \sum_{ij} \tau^{ij} \,. \tag{10}$$

The operator Q_i describes the transition of the state $|\varphi\rangle$ under the action of the potential w_i that is localized at the site $\boldsymbol{R}_i$ in the presence of all the scattering centers w_j, $j \neq i$. The operators τ^{kl}, first introduced by Gyorffy [19, 20], describe the transition of a state $|\varphi'\rangle$ under the action of w_k, where $|\varphi'\rangle$ evolves from $|\varphi\rangle$ after being subjected to w_l. Hence, in (10) the transition of $|\varphi\rangle$ due to the perturbation W is broken down into successive single-site transitions that are computationally more accessible.

For the scattering of correlated systems from the muffin-tin potential W we follow the above ideas by assuming that in absence of W the system $\mathcal{S}$, consisting of N interacting particles, is in a state $|\phi\rangle$. We assume further that in absence of any internal interactions within $\mathcal{S}$, the system is fully described by the state $|\phi_0\rangle$. Usually, this state is given in an explicit form.

Our strategy is to decouple effects due to internal correlation of $\mathcal{S}$ from those arising due the scattering from W. To this end we write the Hamiltonian of the total system, consisting of $\mathcal{S}$ and W, in the form $H = K + \sum_{j>i}^N u_{ij} + \sum_k^M \sum_l^N w_{kl} = K + U_{\text{int}} + W_{\text{ext}}$ where u_{ij} describes the interaction of particle i with particle j within the compound $\mathcal{S}$, w_{kl} is the interaction potential of particle l with the potential centered at the site $\boldsymbol{R}_k$ and K is the kinetic energy operator. The idea now is to decouple dynamical properties due to W_{ext} from those due to U_{int}. To do that we define $w^k := \sum_l w_{kl}$ (the interaction of all N particles with the site $\boldsymbol{R}_k$). The state $|\phi\rangle$ is thus an eigenfunction of $K + U_{\text{int}}$. The system $\mathcal{S}$ goes over into the state $|\Psi\rangle$ when subjected to W_{ext}. This state can be written as

$$\begin{aligned} |\Psi\rangle &= [\mathbf{1} + G_{\text{int}} T_{\text{ext}}] \, |\phi\rangle \\ &= [\mathbf{1} + G_{\text{int}} T_{\text{ext}}] \, [\mathbf{1} + G_{\text{int}} U_{\text{int}}] \, |\phi_0\rangle \,. \end{aligned} \tag{11}$$

Following the procedure for single-particle scattering we can derive an expansion for T_{ext} by noting that (cf. (5))

$$q_{\text{ext}}^k = w^k + w^k G_{\text{int}} q_{\text{ext}}^k + \sum_{l \neq k}^M w^k G_{\text{int}} q_{\text{ext}}^l \,, \tag{12}$$

with $T_{\text{ext}} = \sum_k^M q_{\text{ext}}^k$. Furthermore, we can define the scattering path operator, $\bar{\tau}^{ij}$, of the system $\mathcal{S}$ (for the scattering from W_{ext}) as

$$\bar{\tau}^{ij} = \bar{t}_i \delta_{ij} + \sum_{k \neq i}^M \bar{t}_i G \bar{\tau}_{\text{ext}}^{ik} \,, \tag{13}$$

where $\bar{t}_k = w^k + w^k G_{\text{int}} \bar{t}_k$ is the scattering of the system from the single site k. Equtation 13 describes the scattering of the system $\mathcal{S}$, as a whole, from the multi-center potential W_{ext}. The physical meaning of the operator $\bar{\tau}^{ij}$, q_{ext}^k and $\bar{t}_k$ is just the same as discussed for the single-particle case where the system $\mathcal{S}$ as whole is considered as a "quasi" single particle. The internal response of the system due to the interaction U_{int} is described by $|\phi\rangle = [\mathbf{1} + G_{\text{int}} U_{\text{int}}] |\phi_0\rangle$ that appears in the expression (11) for the total state vector. We note however, that the internal and the external motions are not separable due to the presence of the Green function G_{int} in (12). Till this point

the above exact treatment is just a reformulation of the many-body problem in an integral form. Approximate solutions are deduced from (11) and (13). In the extreme case of weak internal coupling we can neglect $U_{\rm int}$ and arrive at the scattering of independent particles from multi-center potential or we can use in (11) the Dyson expansion of $G_{\rm int}$ for a perturbative approach with regard to $U_{\rm int}$. The first-order expression that contains the involved interactions on equal footing has the form [21]

$$|\Psi\rangle \approx \left[\mathbf{1} + G_0 \bar{T}_{\rm ext}\right] \prod_{j>i}^{N} (\mathbf{1} + u_{ij} g_{ij}) |\phi_0\rangle \,. \tag{14}$$

The transition matrix $\bar{T}_{\rm ext} = W_{\rm ext} + W_{\rm ext} G_0 \bar{T}_{\rm ext}$ can be expressed in terms of the single-site scattering as done in (11). The pair operator g_{ij} is the propagator within the two-body potential u_{ij}. Recent treatments [22, 23] of the two-electron emission from ordered materials following the electron impact can be formally derived from (14).

2 Application to the two-electron emission

In this section we apply the preceding theoretical model to the two-electron emission from a clean perfect surface. For this purpose, further inspection and simplification of (14) is needed.

2.1 One-photon, two-electron transitions

The simplest application of (14) is the emission of two correlated electrons. In this case the product in (14) reduces to only one term corresponding to the inter-electronic potential u_{12}. For a DPE reaction with linear polarized photon, the differential cross section $\mathrm{d}\sigma$ (the transition rate normalized to the incoming photon-flux density) for the emission of two electrons with momenta $\boldsymbol{k}_1$ and $\boldsymbol{k}_2$ is given by [18]

$$\mathrm{d}\sigma = 4\pi^2 \alpha\omega \sum_{\alpha_i} |\langle \Psi | \epsilon \cdot \boldsymbol{D} | i(\alpha_i)\rangle|^2 \, \delta(E_f - E_i) \mathrm{d}\boldsymbol{k}_1 \mathrm{d}\boldsymbol{k}_2 \,. \tag{15}$$

Here α is the fine-structure constant, ω is the frequency of the photon with polarization vector ϵ, $\boldsymbol{D}$ is the dipole operator (in length form), $|i(\alpha_i)\rangle$ is the many-body ground state and $|\Psi\rangle$ is given by (14). Equtation 15 sums over unresolved initial-state quantum numbers α_i. In principle the correlated initial state $|i\rangle$ can be derived in an analogous way from (14) starting from uncorrelated states $|\phi_0\rangle$.

To get an insight into the effects of electronic correlation let us look at the case where $|i\rangle$ describes a many-body localized state, for example a core-level state, from which two fast electrons are emitted (the energies of the vacuum electrons E_1 and E_2 have to be much larger than the binding energies). We assume a frozen-core approximation, i.e., only the degrees of freedom of the two emitted electrons are affected by the photo-absorption process. Furthermore, we inspect cases where the on-site potentials w_i and the final-state internal potentials u_{12} are weak (the electrons are very fast). Under these circumstances the cross section for the DPE can be written as [18]

$$\mathrm{d}\sigma \propto |\boldsymbol{\epsilon} \cdot (\boldsymbol{k}_1 + \boldsymbol{k}_2)|^2 |\tilde{\phi}_i(\boldsymbol{k}_1, \boldsymbol{k}_2)|^2 \delta^{(3)}_{(\boldsymbol{q}_i - \boldsymbol{q}_f, \boldsymbol{G})} \,, \tag{16}$$

where $\boldsymbol{q}_i = \boldsymbol{k}'_1 + \boldsymbol{k}'_2$, $\boldsymbol{q}_f = \boldsymbol{k}_1 + \boldsymbol{k}_2$ are the wave vectors of the pair's center-of-mass in the initial and final state, respectively, i.e. $\boldsymbol{k}'_1$ and $\boldsymbol{k}'_2$ are the initial Bloch wave vectors of the individual electrons. The bulk reciprocal lattice vector is referred to by $\boldsymbol{G}$. $\tilde{\phi}_i(\boldsymbol{k}_1, \boldsymbol{k}_2)$ is the double Fourier transform of the correlated two-electron *Wannier* initial state.

From (16) one can conclude

(a) The delta function in (16) expresses a von Laue-like diffraction condition for the *two electrons* when the center-of-mass momentum of the *pair* changes by a reciprocal bulk lattice vector during the emission process. This (and the selection rules stated below) is equivalent to assuming the pair as a quasi particle with momentum $\boldsymbol{k}_1 + \boldsymbol{k}_2$ (the pair's center-of-mass momentum) and performing a single photoemission of this quasi particle.

(b) The selection rules can be summarized in the equation $\boldsymbol{\epsilon} \cdot (\boldsymbol{k}_1 + \boldsymbol{k}_2) = 0$, i.e. double-photoemission is forbidden if the momentum of the two-electron center-of-mass is perpendicular to the polarization vector or if $\boldsymbol{k}_1 = -\boldsymbol{k}_2$. In addition, the structure of $\tilde{\phi}_i(\boldsymbol{k}_1, \boldsymbol{k}_2)$, which is very much dependent on the symmetry of the investigated core level, imposes additional restrictions on the PDE spectra. In fact, as clear from (16), the structure of $|\tilde{\phi}_i(\boldsymbol{k}_1, \boldsymbol{k}_2)|$ can be probed by a DPE experiment. These conclusions remain valid if we allow for mutual repulsion of the outgoing electrons, but disregard the final-state coupling to the cores [18].

For delocalized states similar conclusions are drawn (see [18] for more details).

2.2 Double electron emission upon electron impact

In this section we consider the simultaneous two-electron emission from delocalized states upon the impact of an electron with momentum $\boldsymbol{k}_0$. The initial state, consisting of an excited electronic vacuum state with wave vector $\boldsymbol{k}_0$ and a bound state $|\chi_{\epsilon(\boldsymbol{k})}\rangle$ with energy ϵ and wave vector $\boldsymbol{k}$ has the asymptotic (long before the collision) form $|\boldsymbol{k}_0, \chi_{\epsilon(\boldsymbol{k})}\rangle$. To calculate the state (14) of the system during the excitation process we assume a screened (renormalized) Coulomb interaction u_{12} for the inter-electronic coupling. Furthermore the explicit shape of the external potential $W_{\rm ext}$ is needed. Here we employ an approximate non-overlapping muffin-tin ionic potentials $w_i^{\rm ion}$ ($W_{\rm ext} = \sum_i w_i^{\rm ion}$) (see [24] for more details). The form factor $\tilde{W}_{\rm ext} := \langle \boldsymbol{p} | W_{\rm ext} | \boldsymbol{k}_0 \rangle$ corresponding to this scattering potential can then be reduced to

$$\tilde{W}_{\rm ext} = \frac{N\sqrt{2\pi}\, f}{A_{\rm uc}} \sum_{\ell} \mathrm{e}^{-\mathrm{i}K_z r_{\perp,\ell}} \sum_{\boldsymbol{g}_\parallel} \delta^{(2)}(\boldsymbol{g}_\parallel - \boldsymbol{K}_\parallel) \tilde{w}^{\rm ion}(\boldsymbol{K}) \,, \tag{17}$$

where $\tilde{w}^{\rm ion}(\boldsymbol{K})$ is the Fourier transform of $w^{\rm ion}$, N is the number of ionic cores illuminated by the electron beam, $A_{\rm uc}$ is the volume of the two-dimensional unit cell, $\boldsymbol{g}_\parallel$ is the surface reciprocal lattice vector, ℓ enumerates the atomic layers with shortest distance $r_{\perp,\ell}$ with respect to the origin, $\boldsymbol{K} = \boldsymbol{p} - \boldsymbol{k}_0$, and $f = \exp(\mathrm{i}\boldsymbol{p} \cdot \boldsymbol{r}_2)$ with $\boldsymbol{r}_2$ refering to the coordinate of the bound electron. With this external potential and the renormalized inter-electronic interaction, the application of (14) yields

for the scattering amplitude [17, 22]

$$\mathcal{T} = T_{12} + T_{\rm ext}. \tag{18}$$

Here T_{12} is a direct electron pair excitation amplitude without any interaction with the crystal whereas $T_{\rm ext}$ involves the scattering of the correlated pair from the crystal potential $W_{\rm ext}$. The amplitude (18) can be written in the explicit form

$$\mathcal{T} = \delta^{(2)}(\boldsymbol{K}^+_{0,\parallel} - \boldsymbol{K}^+_{\parallel})\,\mathcal{L}' + C\sum_{\ell,\boldsymbol{g}_\parallel}\delta^{(2)}\left[\boldsymbol{g}_\parallel - (\boldsymbol{K}^+_{\parallel} - \boldsymbol{K}^+_{0,\parallel})\right] \times \mathcal{L}(\boldsymbol{g}_\parallel, \ell, \boldsymbol{K}^+, \boldsymbol{K}^-, \boldsymbol{k})\,. \tag{19}$$

In (19) $\boldsymbol{K}^+_0 = \boldsymbol{k}_0 + \boldsymbol{k}$ and $\boldsymbol{K}^+ = \boldsymbol{k}_1 + \boldsymbol{k}_2$ are the initial and the final-state wave vector of the pair, respectively. $\boldsymbol{K}^- = \boldsymbol{k}_1 - \boldsymbol{k}_2$ is the inter-electronic wave vectors of the pair. The functions C, $\mathcal{L}$, $\mathcal{L}'$ depend on the description of the momentum-space wave function $\langle \boldsymbol{q}|\chi_{\epsilon(\boldsymbol{k})}\rangle$ of the bound electron. For a jellium-state momentum distribution and free inter-electronic propagation, (19) can be evaluated in closed form [22].

As in the case of DPE, presented in the preceding section, only the pair's center-of-mass wave vector enters in the von Laue-like diffraction condition, i.e. one can regard the pair as a quasi particle located at the pair's center of mass. As in LEED (low energy electron diffraction) studies [24, 25] diffraction occurs when the parallel component of this quasi particle's wave vector is changed by $\boldsymbol{g}_\parallel$ during the collision. However, the pair's diffraction differs decisively from the LEED case. The pair diffraction occurs at a fixed $\boldsymbol{K}^+$. This does not imply fixed $\boldsymbol{k}_1, \boldsymbol{k}_2$ since a momentum exchange of the two electrons (the internal coordinate $\boldsymbol{K}^-$ changes then) does not necessarily modify $\boldsymbol{K}^+$. Therefore, the pair diffraction is actually a manifestation of inter-electronic correlation (otherwise, diffraction of each of the separate electrons will take place). This is in contrast to a LEED reaction where the electronic correlation does not modify significantly the positions of the diffraction beams.

Moreover, whereas the diffraction peaks are determined by the coupling to the crystal potential (and hence depend only on $\boldsymbol{K}^+$), the functional dependence of $\mathcal{L}$ on $\boldsymbol{K}^-$, which characterizes the strength of electronic correlation (in momentum space u_{12} depends only on $|\boldsymbol{K}^-|$), controls the *intensity* of the individual diffraction peaks and the actual shape of the spectra.

The experiments for the two-electron emission via electron impact have been performed in the geometry sketched in Fig. 1. The incoming electron beam is tilted by an angle γ with respect to the normal of the surface whereas the two electrons are emitted under an angle $\pm\alpha$ with respect to surface normal. For a given incident energy, E_0, and a fixed total energy of the pair $E_{\rm tot} = E_1 + E_2$, the coincidence counts are monitored for different energy-sharing, $(E_1 - E_2)/E_{\rm tot}$. To illustrate the diffraction conditions, as anticipated by (19), we note that $\boldsymbol{k}_0, \boldsymbol{k}_1, \boldsymbol{k}_2$ lie in the $x-z$ plane (cf. Fig. 1), i.e. $\boldsymbol{K}^+_\parallel$ possesses only one non-vanishing component K^+_x along the x axis. According to (19), it is this component that is relevant for the pair diffraction and hence we transform the variable $(E_1 - E_2)/E_{\rm tot}$ into K^+_x. In Fig. 2, the pair emission cross section from a Fe(110) (BCC) crystal is shown as function of K^+_x. The cross section is then proportional to $|\mathcal{T}|^2$ (19).

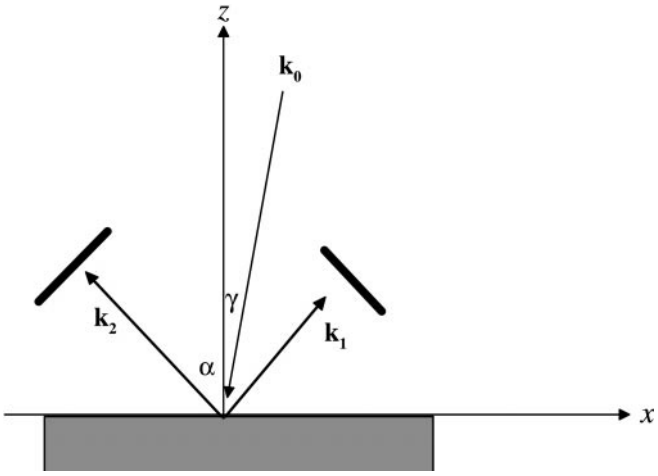

Fig. 1. The experimental setup as used in the experiments shown in Figs. 2, 3

An integration over $\boldsymbol{k}_\parallel$ (weighted with the density of states) and an average of the spin degrees of freedom are, however, necessary since these quantities are not experimentally resolved [22].

Assuming $\boldsymbol{k}_\parallel = 0$, the positions of the first diffraction maxima (hereafter referred to as the $(-1, 0)$ $(1, 0)$ maxima) are indicated by arrows. The theoretical and experimental data (Fig. 2) clearly show the (1,0), and $(-1, 0)$ diffraction peaks. The asymmetric shape of the spectrum is due to the broken symmetry of the experiment since the incoming beam does not coincide with the normal of the surface ($\gamma = 5°$).

In Fig. 3a–c we choose $\gamma = 0$ and a Cu(001) crystal as a target. The spectra become then symmetric with respect to $E_1 = E_2$ since the whole experimental setup (the scattering plane, spanned by $\boldsymbol{k}_1$ and $\boldsymbol{k}_2$, and the crystal) is invariant under a 180° rotation around $\hat{\boldsymbol{z}}$ (note that $\boldsymbol{k}_0 \parallel \hat{\boldsymbol{z}}$ lies in the scattering plane and is the bisector of the relative angle $\cos^{-1}(\hat{\boldsymbol{k}}_1 \cdot \hat{\boldsymbol{k}}_2)$). To illustrate the exchange coupling between the two emitted electrons we inspect in Fig. 3a the singlet (dotted curve

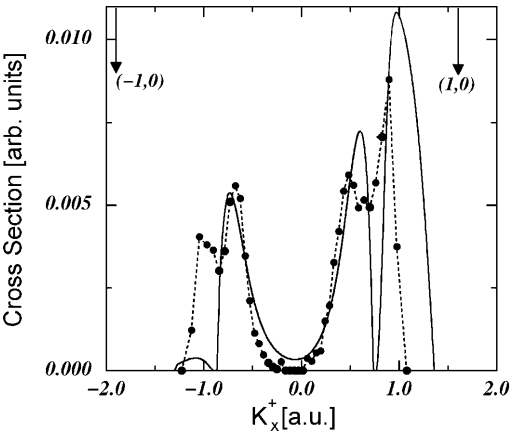

Fig. 2. The experimental results (*full dots*) for a Fe(110) (BCC) sample at an incident energy of 50 eV. The total energy of the pair is $E_{\rm tot} = E_1 + E_2 = 44$ eV. The incident beam is tilted with respect to the normal by an angle of $\gamma = 5°$ (cf. Fig. 1) and $\alpha = 50°$. The *solid curve* shows the theoretical results. The experimental results are on a relative scale

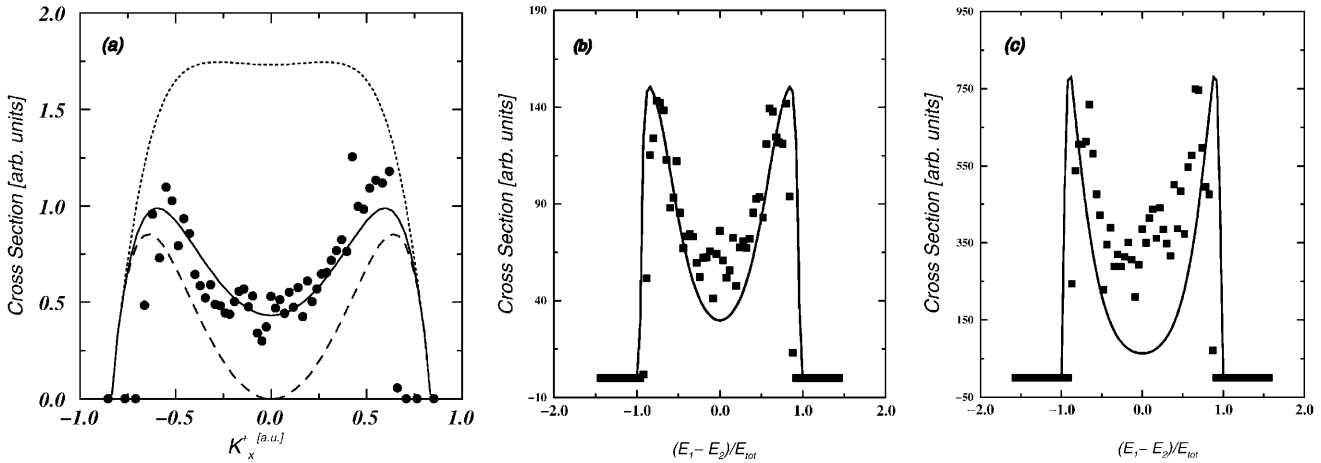

Fig. 3a–c. The same as in Fig. 2 for a Cu(001) crystal in the normal incidence geometry that corresponds to $\gamma = 0$ in Fig. 1. Furthermore we choose $\alpha = 40°$ (cf. Fig. 1). The incident energy is $E_i = 34$ eV and $E_{\rm tot} = 27$ eV. The singlet, σ^s, (*dotted curve*) and the triplet, σ^t, (*dashed curve*) scattering cross sections are shown along with their statistical average, $0.25\sigma^s + 0.75\sigma^t$, (*solid curve*). The relative spin non-resolved experimental data (*full dots*) are shown. They have been normalized to theory at one point. **b**, **c** We use the same target, scattering geometry, and incident energy as in **a**. However, the total energy of the pair is lowered to $E_{\rm tot} = 25$ eV and $E_{\rm tot} = 23$ eV in **b** and **c**, respectively. In all cases the experiments have been performed by the group of Prof. Kirschner [26]

in Fig. 3a) and the triplet (dashed curve in Fig. 3a) scattering contribution to the spin non-resolved spectrum (solid curve in Fig. 3a). From simple symmetry consideration one can conclude that the triplet scattering must vanish when the two electrons emerge with the same energies, i.e. for $K_x^+ = 0$. In fact, within our (approximate) model, it seems that the minimum in the spin-averaged spectrum around $K_x^+ = 0$ is caused primarily by the diminishing triplet contribution at $K_x^+ = 0$.

In Fig. 3b,c the energy-sharing distributions are depicted for various total energies of the pair $E_{\rm tot}$. This means that the electron pairs originate from various states in the conduction band. For electron emission from states close to the bottom of the band the agreement between theory and experiment worsens. This is due to the contribution of other channels for the production of electron pairs in which the emission of the pair is accompanied by inelastic processes. Presently, such channels are not accounted for by the theory. A more elaborate treatment taking inelastic reactions into account and employing a more realistic potential than the one given in (17) is in progress.

3 Conclusions

In this work we studied the electron-pair emission from solids and surfaces. We discussed a formal theory for the treatment of correlated system as they propagate through a multi-center potential. The simplest case of two correlated electrons, produced by electron and photon impact from a perfect surface, has been considered.

Acknowledgements. I would like to thank Profs. J. Kirschner, R. Feder, P. Bruno, and O.M. Artamonov as well as Drs. S. Samarin and H. Gollisch for many stimulating discussions and suggestions.

References

1. A.H. Wilson: Proc. Roy. Soc. A **133**, 458 (1931)
2. W. Kohn, L.J. Sham: Phys. Rev. A **140**, 1133 (1965)
3. J. Hubbard: Proc. Roy. Soc. A **277**, 237 (1964)
4. P.W. Anderson: Phys. Rev. **124**, 41 (1961)
5. L. Sangaletti, F. Parmigiani, T. Thio, J.W. Bennett: Phys. Rev. B **55**, 9514 (1997)
6. A. Fujimori, F. Minami: Phys. Rev. B **30**, 957 (1984)
7. A. Fujimori, M. Saeki, N Kimizuka, M. Taniguchi, S. Suga: Phys. Rev. B **34**, 7318 (1986)
8. J. van Elp, H. Eskes, G.A. Sawatzky: Phys. Rev. B **45**, 1612 (1992)
9. J. Braun: Rep. Prog. Phys. **59**, 1267 (1996)
10. R. Herrmann, S.N. Samarin, H. Schwabe, J. Kirschner: Phys. Rev. Lett. **81**, 2148 (1998)
11. I.E. McCarthy, E. Weigold: Rep. Prog. Phys. **54**, 789 (1991)
12. M. Vos, I.E. McCarthy: Rev. Mod. Phys. **67**, 713 (1995)
13. A.S. Kheifets, S. Iacobucci, A. Ruoccoa, R. Camilloni, G. Stefani: Phys. Rev. B **57**, 7380 (1998)
14. J. Kirschner, O.M. Artamonov, A.N. Terekhov: Phys. Rev. Lett. **69**, 1711 (1992)
15. J. Kirschner, O.M. Artamonov, S.N. Samarin: Phys. Rev. Lett. **75**, 2424 (1995)
16. O.M. Artamonov, S.N. Samarin, J. Kirschner: Appl. Phys. A **65**, 535 (1997)
17. J. Berakdar, S.N. Samarin, R. Herrmann, J. Kirschner: Phys. Rev. Lett. **81**, 3535 (1998)
18. J. Berakdar: Phys. Rev. B **58**, 9808 (1998)
19. B.L. Gyorffy: *Fondamenti Di Fisica Dello Stato Solida* (Scuola Nazionale di Struttura della Materia 1971)
20. B.L. Gyorffy, M.J. Stott: In *Bandstructure Spectroscopy of Metals and Alloys*, ed. by D.J. Fabian, L.M. Watson (Academic Press, London 1973)
21. J. Berakdar: unpublished (1999)
22. J. Berakdar, M.P. Das: Phys. Rev. A **56**, 1403 (1997)
23. H. Gollisch, G. Meinert, X. Yi, R. Feder: Solid State Commun. **102**, 317 (1997)
24. J.B. Pendry: *Low Energy Electron Diffraction* (Academic Press, London 1974)
25. M.A. van Hove, W.H. Weinberg, C.-M. Chan: *Low Energy Electron Diffraction*, Springer Series in Surf. Sci. (Springer, Berlin, Heidelberg 1986)
26. S.N. Samarin, O.M. Artamonov, J. Kirschner: private communication